Applications of Effective Core Potentials and Density Functional Theory to the Spin States of Iron Porphyrin

Yi-Ping Liu[1]

Department of Chemistry, Western Michigan University, Kalamazoo, Michigan 49008

Received June 5, 2000

We investigated the performance of the B3LYP density functional in combination with ab initio effective core potentials (ECPs) that are derived from either Hartree−Fock or Dirac−Fock calculations. The transferability of ab initio ECPs is assessed on the basis of comparison with all-electron density functional calculations. For iron(II) porphyrin in particular, our assessment focused on the relative energetic ordering of five low-lying spin states, $^1A_{1G}$, $^3A_{1G}$, $^3B_{2G}$, $^5A_{2G}$, and $^5B_{1G}$, and their properties, including optimized structures, charge distribution, spin density, and vibrational frequencies. Our results show that core electron correlation and core−valence electron correlation do not have significant effects on the relative energetics of the spin states of iron porphyrin. Our calculations suggest that effects of replacing the core electrons with ECPs are less significant than the choice of basis functions. We conclude that ab initio ECPs such as LANL2, RCEP, and MEFIT-R may be combined with the B3LYP density functional theory to provide consistent and accurate results.

I. INTRODUCTION

The difficulties of treating transition metal compounds with *ab initio* molecular orbital methods have been well documented.[1] Spin−orbit couplings and relativistic effects are often nonnegligible for transition metals. The manifold of close-lying electronic states and the tightly packed electrons in the d shell in transition metals give rise to significant static and dynamic electron correlation and, as a result, escalate the computational cost.

A recent trend in theoretical treatment of transition metals is the fusion of ab initio effective core potentials and density functional theories. Density functional theories (DFT) afford the inclusion of electron correlation at modest computational cost.[1−4] The B3LYP parametrization of DFT in particular has demonstrated reasonable accuracy for many molecular systems. In the ab initio effective core potential (ECP) methods, only the valence electrons are treated explicitly. The effects of the core electrons on the valence electrons are represented by a set of effective core potentials which are obtained by fitting to, for example, the atomic orbital energies or valence energies, and/or orbital shape from all-electron calculations. In fitting the ECPs, spin−orbit couplings and relativistic effects may be implicitly included, depending on the Hamiltonians used in the fitting procedure.

A common practice in combining a particular type of density functional with ECPs is to use an ECP fitted to all-electron calculations using the same density functional. This ensures consistency in the treatment of electron correlation for the valence and the core electrons. To exploit ab initio effective core potentials in calculations based on density functional theories, one therefore has to address the question whether ab initio effective core potentials are transferable. Russo, Martin, and Hay compared binding energies and bond lengths for compounds of Sc, Ti, V, Ni, and Cu calculated from BLYP/ab initio ECPs and from all-electron BLYP calculations.[5] Glukhovtsev, Bach, and Nagel[6] compared experimental bond strength of iron-containing compounds and values calculated using B3LYP and ab initio ECPs of Dolg, Wedig, Stoll, and Preuss.[7]

In this work, we assess the transferability of ab initio ECPs on the basis of comparison with all-electron density functional calculations. For iron(II) porphyrin in particular, our assessment focuses on the relative energetic ordering of five low-lying spin states, $^1A_{1G}$, $^3A_{1G}$, $^3B_{2G}$, $^5A_{2G}$, and $^5B_{1G}$, and their properties. Iron porphyrin is part of the active sites of many important enzymes. It has been shown experimentally and theoretically that catalytic functions are often closely coupled to the spin states.[8,9] Our results can therefore shed light on the validity and accuracy of combining DFT with ab initio ECPs in modeling spin-state modulation of enzyme functions.

II. METHODS

In all calculations using ECPs, electrons in the completely filled 3s and 3p sub shells were considered valence electrons. Three effective core potentials were compared: (1) LANL2, derived from all-electron numerical Hartree−Fock atomic wave functions by Wadt and Hay;[10] (2) RCEP, derived from numerical Dirac−Fock calculations of appropriate atomic configurations by Stevens, Krauss, Basch, and Jasien;[11] and (3) MEFIT-R, a set of quasi-relativistic ECPs derived from both the nonrelativistic and relativistic Hartree−Fock valence energies of configurations of the one-valence electron ion Fe^{15+} by Dolg, Wedig, Stoll, and Preuss.[7]

For calculations carried out with the ECPs, the corresponding energy-optimized basis functions for iron were used. The LANL2 energy-optimized basis functions for iron consist of three s, three p, and two d orbitals contracted from

* E-mail: yi-ping.liu@wmich.edu. Phone: 616-387-2865.

10.1021/ci000051f CCC: $20.00
Published on Web 10/21/2000

Table 1. Basis Functions

	effective core potential			all-electron		
	LANL2	RCEP	MEFIT-R	SVP	TZV	Wachters
Fe	double-ζ[a]	triple-ζ[b]	(8s7p6d1f)/[6s5p3d1f][c]	(14s9p5d)/[5s3p2d][d]	(17s10p6d)/[6s3p3d][e]	(14s9p5d)/[8s5p3d][f]
C, N, H	valence double-ζ[g]	6-31G	full double-ζ[h]	6-31G(d)	6-31G(d)	6-31G(d)
number of primitive Gaussians	701	644	699	791	803	791
number of basis functions	262	271	313	384	390	399

[a] References 10 and 12. [b] References 11 and 13. [c] Reference 7. [d] Reference 14. This is the SV basis set 14s8p5d)/[5s2p2d] with an extra p function added for polarization. [e] Reference 15. [f] References 16 and 17. [g] Reference 18. [h] Reference 18.

Table 2. Relative Spin State Energies (in eV)

	ECP, single point[a]			ECP[b]			all-electron[b]		
	LANL2	RCEP	MEFIT-R	LANL2	RCEP	MEFIT-R	SVP	TZV	Wachters
$^1A_{1G}$	1.42	1.48	1.49	1.40	1.48	1.48	1.56	1.55	1.68
$^5B_{1G}$	0.67	0.62	0.53	0.65	0.64	0.53	0.61	0.77	0.76
$^3B_{2G}$	0.57	0.56	0.55	0.51	0.53	0.49	0.63	0.56	0.69
$^5A_{2G}$	0.28	0.19	0.14	0.23	0.17	0.08	0.21	0.30	0.27
$^3A_{1G}$	0.00	0.00	0.00	0.00	0.00	0.00	0.00	0.00	0.00

[a] Single-point calculations at geometries optimized in all-electron calculations using Wachters basis functions for iron. The ECPs and the corresponding energy-optimized basis functions were used for iron. The 6-31G(d) basis set for other atoms as in the all-electron calculations. [b] Energies at equilibrium geometries calculated using basis functions specified in Table 1.

the corresponding type of primitive Gaussian functions (five primitives of each type).[10,12] The RCEP basis functions for iron consist of four sets of contracted sp orbitals and three contracted d orbitals. The sp orbitals of the $n = 3$ shell are expansions of four and one Gaussian functions, respectively. The sp orbitals of the $n = 4$ shell are expansions of two and one Gaussian functions, respectively. The d orbitals are of a triple-ζ type based on the contraction scheme: four, one, and one Gaussian functions.[11,13] The MEFIT-R energy-optimized basis functions consist of six s, five p, three d, and one f orbitals contracted from eight s, seven p, six d and one f Gaussian type orbitals.[7]

To gauge the effects of basis functions, we used three different basis functions for iron in the all-electron calculations: the split-valent basis set of Schäfer, Horn, and Ahlrichs[14] with polarization (denoted as SVP), the triple-ζ basis set of Schäfer, Huber, and Ahlrichs[15] (denoted as TZV), and the basis set from Wachters[16,17] which consists of eight s, five p, and three d orbitals contracted from fourteen s, nine p, and five d Gaussian type orbitals.

For all-electron calculations, we used the 6-31G(d) basis set for carbon, nitrogen, and hydrogen. For direct comparison between calculations with and without ECPs, the 6-31G(d) basis set for carbon, nitrogen, and hydrogen was employed in ECP calculations to obtain single point energies of each spin state, at geometries optimized in all-electron calculations using Wachters basis functions for iron. The basis sets for carbon, nitrogen, and hydrogen used with each type of ECPs in *all other* calculations are as follows. In calculations using the LANL2 effective core potential, we use the Dunning/Huzinaga valence double-ζ basis[18] for C, N, and H. In the calculations using the RCEP ECPs, we used the 6-31G basis set for C, N, and H. In calculations using the MEFIT-R effective core potential, we used the Dunning/Huzinaga full double-ζ[18] basis functions for C, N, and H. The total number of basis functions and the type of basis functions used are summarized in Table 1.

During geometry optimization, the structure is constrained to have a D_{4h} symmetry. Vibrational frequencies are calculated using the harmonic approximation. All calculations (single-point, geometry optimization, and frequency calculations) were carried out using the B3LYP functional at the unrestricted level except for the singlet states which were calculated at the restricted level. All calculations were carried out using the Gaussian 98 program suite.[19]

III. RESULTS

We first compare energies of spin states $^1A_{1G}$, $^5B_{1G}$, $^3B_{2G}$, and $^5A_{2G}$ relative to that of $^3A_{1G}$. The partially filled molecular orbitals of the low-lying spin states $^1A_{1G}$, $^3A_{1G}$, $^3B_{2G}$, $^5A_{2G}$, and $^5B_{1G}$ correspond primarily to the d orbitals of iron:

spin states	molecular orbitals				
	B_{1G} d_{x2-y2}	A_{1G} d_{z2}	B_{2G} d_{xy}	E_G d_{yz}	E_G d_{xz}
$^1A_{1G}$:	—	—	↑↓	↑↓	↑↓
$^5B_{1G}$:	↑	↑	↑↓	↑	↑
$^3B_{2G}$:	—	↑	↑	↑↓	↑↓
$^5A_{2G}$:	↑	↑↓	↑	↑	↑
$^3A_{1G}$:	—	↑↓	↑↓	↑	↑

Results tabulated in columns 2−4 of Table 2 are single-point energies using the LANL2, RCEP, and MEFIT-R ECPs calculated at geometries optimized in all-electron calculations using Wachters basis functions for iron. In these calculations, the corresponding energy-optimized basis functions were used for iron, and the 6-31G(d) basis set was used for the other atoms as in the all-electron calculations. The calculations presented in columns 2−4 therefore differ from those in the last column (labeled Wachters) in the treatment of core electrons (i.e., without or with the ECPs) and in the basis functions for iron.

The results tabulated in columns 5−10 of Table 2 were obtained using the basis functions specified in Table 1. The

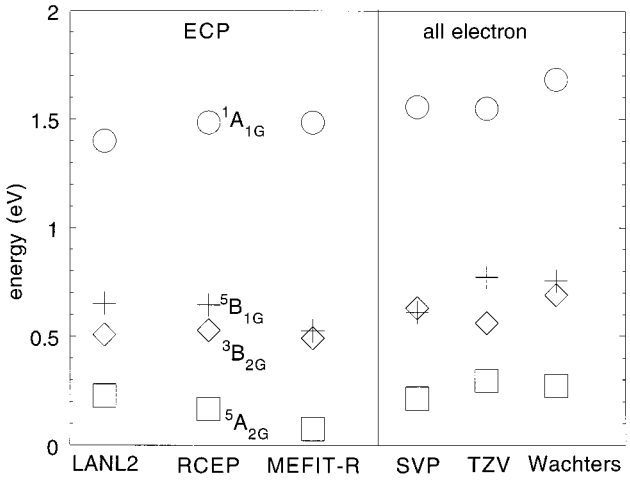

Figure 1. Spin state energy relative to the $^3A_{1G}$ states. Circles denote the $^1A_{1G}$ states, crosses denote the $^5B_{1G}$ states, diamonds denote the $^3B_{2G}$ states, and squares denote the $^5A_{2G}$ states. LANL2, RCEP, and MEFIT-R designate results based on the LANL2, RCEP, and MEFIT-R ECPs, respectively, and the basis functions summarized in Table 1. SVP, TZV, and Wachters designate all-electron results using basis functions summarized in Table 1. The data plotted in this figure are tabulated in Table 2.

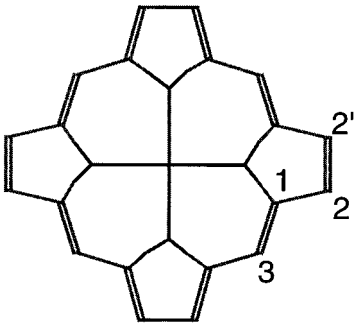

Figure 2. Structure and atomic labels of iron(II) porphyrin.

geometries used in these calculations were individually optimized for each spin state. Results presented in column 2 therefore differ from those in column 5 in the geometries and the basis functions for C, N, and H. The results in columns 5−10 of Table 2 are presented graphically in Figure 1.

The bond lengths in the pairs of atoms Fe−N, Fe−C_3, N−C_1, C_1−C_2, C_2−C_2', C_1−C_3, C_2−H, and C_3−H (see Figure 2 for the definition of atomic labels) completely specify the geometry of iron(II) porphyrin with a D_{4h} symmetry. In Figure 3, we compare the geometries optimized using the ECPs (LANL2, RCEP, and MEFIT-R) with those from all-electron calculations using Wachters basis functions. For the aforementioned bond lengths specifically, we show the *deviations* of the former from those of the latter. In Figure 4, we compare optimized geometries of all-electron calculations using the SVP and TZV basis functions and those obtained in all-electron calculations using Wachters basis functions. As in Figure 3, we show the *deviations* of bond lengths of the former from those of the latter. Compared to the all-electron calculations using Wachters basis functions, bond lengths of all the spin states calculated with ECPs are in agreement to within 0.01 Å except for those for Fe−C_3, N−C_1, C_1−C_2, and C_2−C_2'. These bond lengths are tabulated for all the spin states in Table 3. For completeness, we also

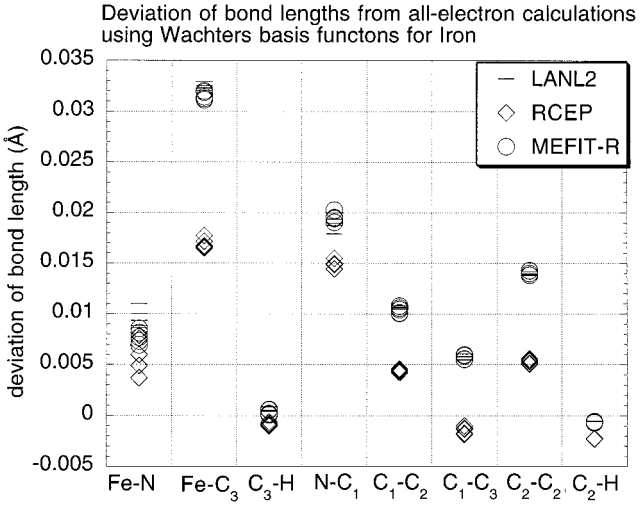

Figure 3. Bond length comparison. The *y* axis is the *difference* of bond lengths from all-electron calculations using Wachters basis functions for iron. Circles, diamonds, and bars represent results using the MEFIT-R, RCEP, and LANL2 ECPs. Basis functions used in these calculations are specified in Table 1.

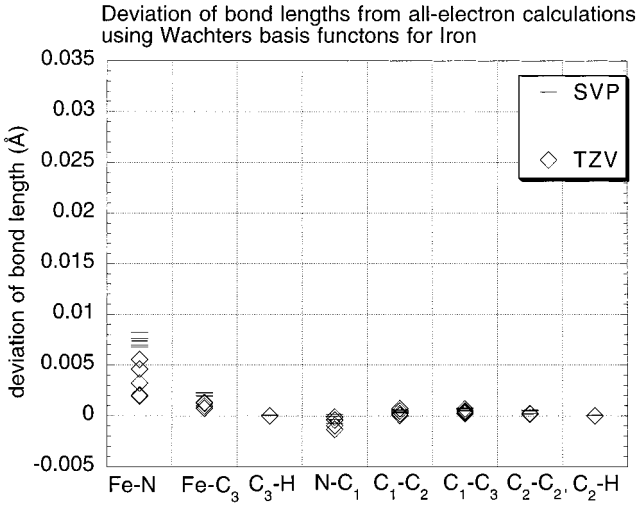

Figure 4. Bond length comparison. The *y* axis is the *difference* of bond lengths from all-electron calculations using Wachters basis functions for iron. Diamonds and bars represent results using the TZV and SVP basis functions. Complete specification of the basis functions used in these calculations is given in Table 1.

listed all bond lengths of the ground spin state $^3A_{1G}$ in Table 4.

The spin density is, as expected, concentrated on iron. The spin density of the ground spin state $^3A_{1G}$ is presented in Table 5. In Table 6, we present the spin density on iron for all the spin states except for the singlet states.

In Figures 5 and 6, we compare Mulliken charges. In both figures, the values from all-electron calculations using Wachters basis functions are used as the ordinate, and the difference from these values is plotted as the abscissa. Results calculated using the three types of ECPs are shown in Figure 5, and the all-electron calculations with different basis functions are compared in Figure 6. The results of the three ECPs are comparable, with the RCEP values closest to the all-electron calculations using the Wachters basis set.

In Figures 7 and 8, we compare atomic charges derived by fitting to the electrostatic potentials. Again in both figures,

Table 3. Selected Bond Lengths (in Å) of Five Spin States[a,b]

	ECP			all-electron		
	LANL2	RCEP	MEFIT-R	SVP	TZV	Wachters
			$^5B_{1G}$			
Fe−C_3	3.471	3.455	3.470	3.440	3.439	3.438
N−C_1	1.393	1.388	1.393	1.373	1.373	1.373
C_1−C_2	1.457	1.451	1.457	1.446	1.446	1.446
C_2−$C_{2'}$	1.380	1.371	1.380	1.366	1.366	1.366
			$^5A_{2G}$			
Fe−C_3	3.471	3.455	3.470	3.441	3.439	3.438
N−C_1	1.392	1.387	1.392	1.372	1.372	1.372
C_1−C_2	1.457	1.450	1.457	1.446	1.446	1.446
C_2−$C_{2'}$	1.379	1.370	1.379	1.366	1.365	1.365
			$^3B_{2G}$			
Fe−C_3	3.453	3.438	3.452	3.423	3.422	3.421
N−C_1	1.397	1.394	1.398	1.379	1.378	1.379
C_1−C_2	1.452	1.446	1.452	1.442	1.442	1.441
C_2−$C_{2'}$	1.374	1.365	1.374	1.360	1.360	1.360
			$^3A_{1G}$			
Fe−C_3	3.454	3.438	3.453	3.424	3.423	3.422
N−C_1	1.396	1.392	1.397	1.377	1.377	1.377
C_1−C_2	1.451	1.445	1.451	1.441	1.441	1.441
C_2−$C_{2'}$	1.375	1.367	1.375	1.362	1.362	1.362
			$^1A_{1G}$			
Fe−C_3	3.453	3.438	3.452	3.423	3.422	3.421
N−C_1	1.396	1.393	1.397	1.377	1.377	1.378
C_1−C_2	1.453	1.447	1.452	1.443	1.443	1.442
C_2−$C_{2'}$	1.374	1.366	1.375	1.361	1.360	1.360

[a] For definition of atomic labels, see Figure 2. [b] Basis functions are specified in Table 1.

Table 4. $^3A_{1G}$ Bond Lengths (in Å)[a,b]

	ECP			all -electron		
	LANL2	RCEP	MEFIT-R	SVP	TZV	Wachters
Fe−N	2.009	2.005	2.007	2.007	2.002	1.999
Fe−C_3	3.454	3.438	3.453	3.424	3.423	3.422
N−C_1	1.396	1.392	1.397	1.377	1.377	1.377
C_1−C_2	1.451	1.445	1.451	1.441	1.441	1.441
C_1−C_3	1.394	1.387	1.394	1.389	1.388	1.388
C_2−$C_{2'}$	1.375	1.367	1.375	1.362	1.362	1.362
C_2−H	1.082	1.080	1.082	1.083	1.083	1.083
C_3−H	1.086	1.085	1.086	1.086	1.086	1.086

[a] For definition of atomic labels, see Figure 2. [b] Basis functions are specified in Table 1.

Table 5. $^3A_{1G}$ Spin Density[a,b]

	ECP			all-electron		
	LANL2	RCEP	MEFIT-R	SVP	TZV	Wachters
Fe	2.02	2.04	2.04	2.04	2.01	2.00
N	−0.04	−0.06	−0.05	−0.05	−0.04	−0.04
C_1	0.02	0.02	0.02	0.02	0.02	0.02
C_2	0.01	0.01	0.01	0.01	0.01	0.01
H(C_2)	0.00	0.00	0.00	0.00	0.00	0.00
C_3	−0.01	−0.01	−0.01	−0.01	−0.01	−0.01
H(C_3)	0.00	0.00	0.00	0.00	0.00	0.00

[a] For definition of atomic labels, see Figure 2. [b] Basis functions are specified in Table 1.

the values from all-electron calculations using Wachters basis functions are used as the ordinate and the difference from these values is plotted as the abscissa.

In Figure 9, we compare vibrational frequencies from all-electron calculations for the ground spin state $^3A_{1G}$. The vibrational frequencies from all-electron calculations using the Wachters basis are used as the ordinate, and the difference from these values is plotted as the abscissa. Figure 9 shows that the deviation in vibrational frequencies due to basis functions is less than 5 cm^{-1} for the most part, and only one vibrational mode exhibits a deviation of nearly 15 cm^{-1}. Similarly in Figure 10, the abscissa represents the deviation of the ECP frequencies from the all-electron calculations using the Wachters basis, for the ground spin state $^3A_{1G}$. In contrast to Figure 9, the deviation shown in Figure 10 spreads over a wider range, with noticeably large deviations (>40 cm^{-1}) for several vibrational modes between 860 and 1000 cm^{-1}. It is also interesting to note that the three ECPs exhibit a similar pattern of deviation.

Figures 11 and 12 contain similar information for the first excited spin state $^5A_{2G}$. The deviation due to basis functions (SVP and TZV vs Wachters, Figure 11) in this case is greater than that for $^3A_{1G}$. Nonetheless, these deviations are within

Table 6. Spin Density on Fe[a]

	ECP			all-electron		
	LANL2	RCEP	MEFIT-R	SVP	TZV	Wachters
$^5B_{1G}$	3.76	3.83	3.83	3.85	3.77	3.83
$^5A_{2G}$	3.70	3.78	3.78	3.75	3.71	3.72
$^3B_{2G}$	2.16	2.20	2.19	2.21	2.17	2.19
$^3A_{1G}$	2.02	2.04	2.04	2.04	2.01	2.00

[a] Basis functions are specified in Table 1.

Table 7. $^3A_{1G}$ IR Active Modes (in cm^{-1})[a]

	ECP			all -electron		
	LANL2	RCEP	MEFIT-R	SVP	TZV	Wachters
A_{2U}	363	363	365	351	351	358
E_U	758	767	758	758	759	759
A_{2U}	803	800	804	782	784	785
A_{2U}	920	922	923	880	877	876
E_U	1011	1019	1009	1022	1021	1024
E_U	1097	1115	1098	1092	1092	1093
E_U	3282	3284	3282	3264	3264	3264

[a] Basis functions are specified in Table 1.

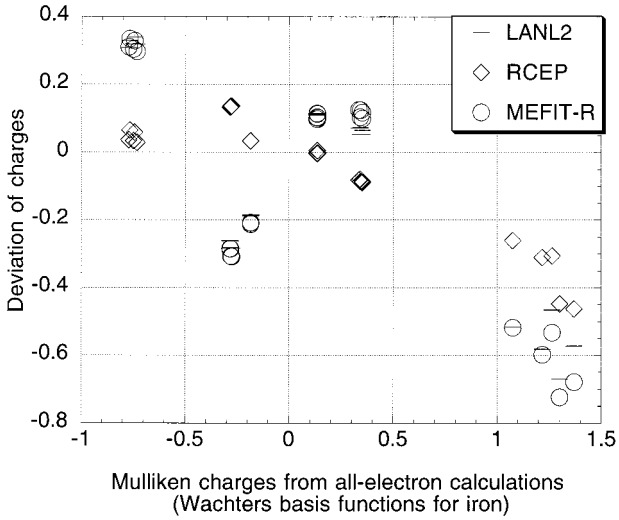

Figure 5. Comparison of Mulliken charges. The Mulliken charges from all-electron calculations using Wachters basis functions are plotted as the ordinate. The *difference* from these values is taken as the abscissa. Circles, diamonds, and bars represent results using the MEFIT-R, RCEP, and LANL2 ECPs. Basis functions used in these calculations are specified in Table 1.

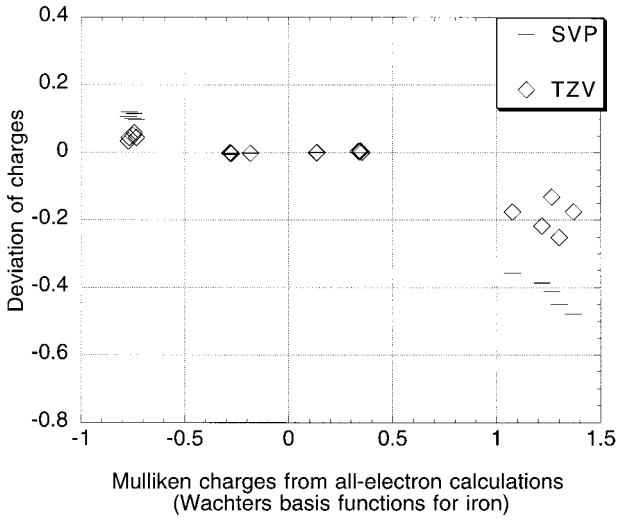

Figure 6. Comparison of Mulliken charges. The Mulliken charges from all-electron calculations using Wachters basis functions are plotted as the ordinate. The *difference* from these values is taken as the abscissa. Diamonds and bars represent results using the TZV and SVP basis functions. Complete specification of the basis functions used in these calculations is given in Table 1.

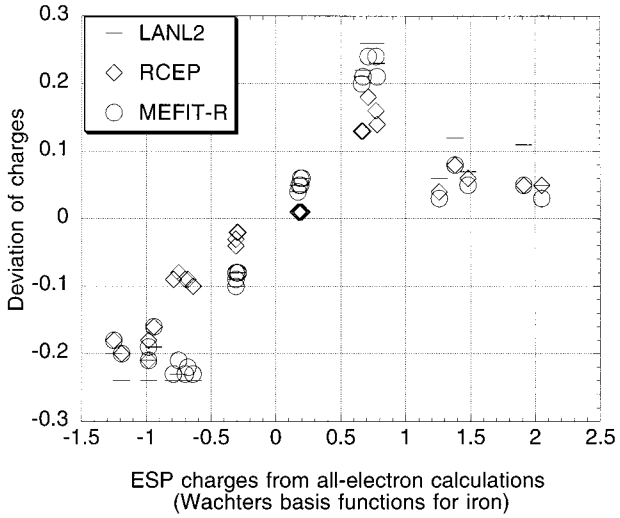

Figure 7. Comparison of charges derived from fitting the electrostatic potential (ESP). The ESP charges from all-electron calculations using Wachters basis functions are plotted as the ordinate. The *difference* from these values is taken as the abscissa. Circles, diamonds, and bars represent results using the MEFIT-R, RCEP, and LANL2 ECPs. Basis functions used in these calculations are specified in Table 1.

20 cm^{-1} for the most part. Again, a greater spread is observed when the ECP vibrational frequencies are compared with those of all-electron calculations using the Wachters basis set (Figure 12). As observed for the $^3A_{1G}$ state, the vibrational modes between 860 and 1000 cm^{-1} again exhibit noticeable large deviations (greater than 40 cm^{-1}). These modes involve mainly the out-of-plane bending motion of C_2-H and $C_{2'}-H$ in the opposite directions and/or the out-of-plane bending motion of C_3-H.

IV. DISCUSSION

The ground state energies of atomic Fe calculated using the basis functions SVP and TZV differ from those using Wachters basis functions by 2.7 and 1.8 eV, respectively.[14,15]

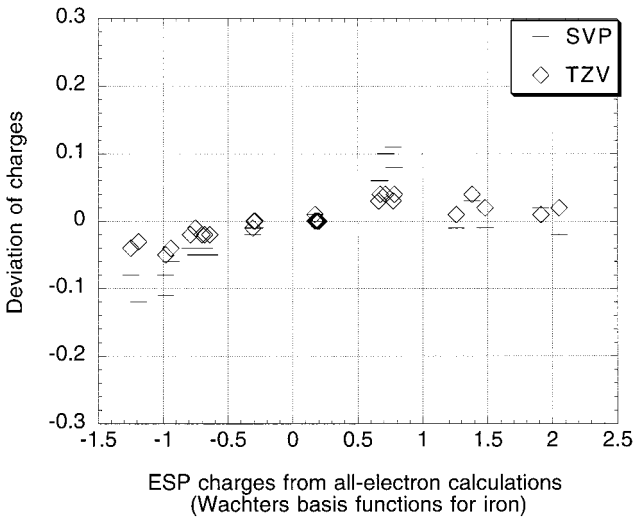

Figure 8. Comparison of charges derived from fitting the electrostatic potential (ESP). The ESP charges from all-electron calculations using Wachters basis functions are plotted as the ordinate. The *difference* from these values is taken as the abscissa. Diamonds and bars represent results using the TZV and SVP basis functions. Complete specification of the basis functions used in these calculations is given in Table 1.

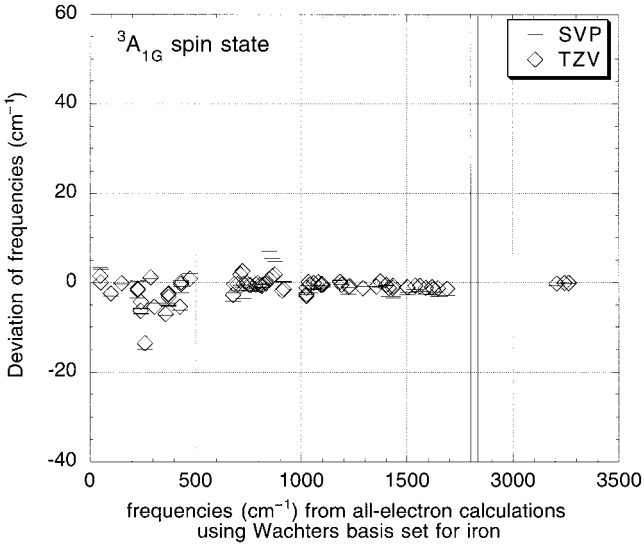

Figure 9. Comparison of frequencies of $^3A_{1G}$ spin state. The frequencies from all-electron calculations using Wachters basis functions are plotted as the ordinate. The *difference* from these values is taken as the abscissa. Diamonds and bars represent results using the TZV and SVP basis functions. Complete specification of the basis functions used in these calculations is given in Table 1.

These discrepancies are largely canceled in the relative spin state energies listed in Table 2 (columns 8−10), and the SVP and TZV results deviate from the calculations using Wachters basis functions by at most 0.16 eV.

Before the calculations with and without ECPs are compared, it is worth noting how the ab initio ECPs are derived and how they differ. In general, the ECPs are represented by a series of terms containing Gaussian functions: $\sum_k d_k r^{n_k} \exp(-\zeta_k r^2)$. The LANL2 ECPs for iron are derived from numerical atomic Hartree−Fock calculations. Wadt and Hay included the relativistic mass−velocity and Darwin effects in the LANL2 ECPs for *heavy* transition metals ($Z > 36$) but *not* for iron.[10] The RCEPs are derived from the numerical Dirac−Fock calculations, and therefore

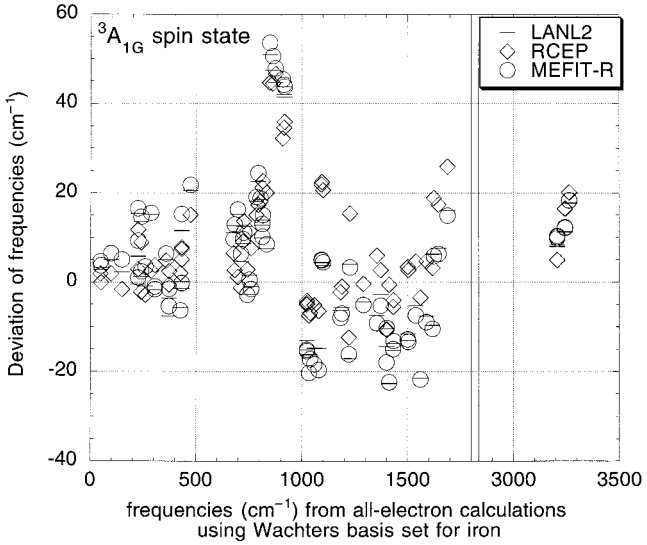

Figure 10. Comparison of frequencies of $^3A_{1G}$ spin state. The frequencies from all-electron calculations using Wachters basis functions are plotted as the ordinate. The *difference* from these values is taken as the abscissa. Circles, diamonds, and bars represent results using the MEFIT-R, RCEP, and LANL2 ECPs. Basis functions used in these calculations are specified in Table 1.

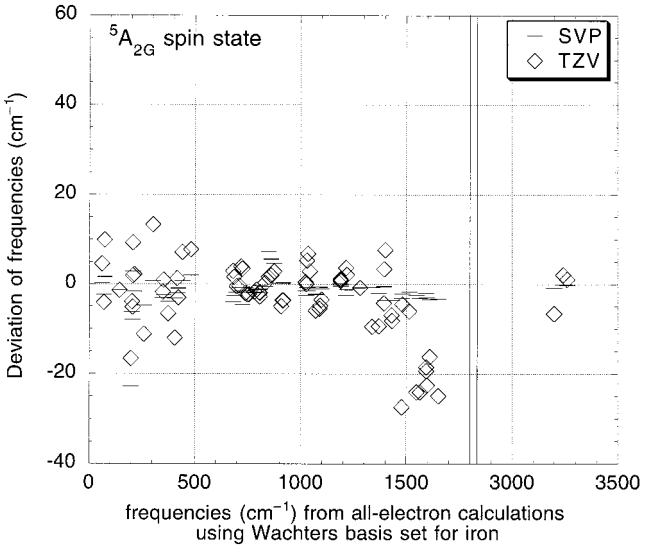

Figure 11. Comparison of frequencies of $^5A_{2G}$ spin state. The frequencies from all-electron calculations using Wachters basis functions are plotted as the ordinate. The *difference* from these values is taken as the abscissa. Diamonds and bars represent results using the TZV and SVP basis functions. Complete specification of the basis functions used in these calculations is given in Table 1.

incorporate implicitly the relativistic effects. The parameters in the MEFIT-R ECPs are first fitted to the nonrelativistic Hartree−Fock valence energies of configurations of the one-valence-electron ion, Fe^{15+}. The exponents of the Gaussian terms are then fixed, and the expansion coefficients are adjusted in a fitting procedure that includes relativistic Hartree−Fock valence energies of the one-valence-electron ion, Fe^{15+}. Valence energies of atomic Fe calculated with MEFIT-R ECPs agree with relativistic Hartree−Fock calculations to within 0.1 eV.[7]

Since the all-electron calculations in the present work do not include relativistic effects, we expect that the incompatibility between ab initio ECPs and DFT should manifest unambiguously in comparison with results using B3LYP/

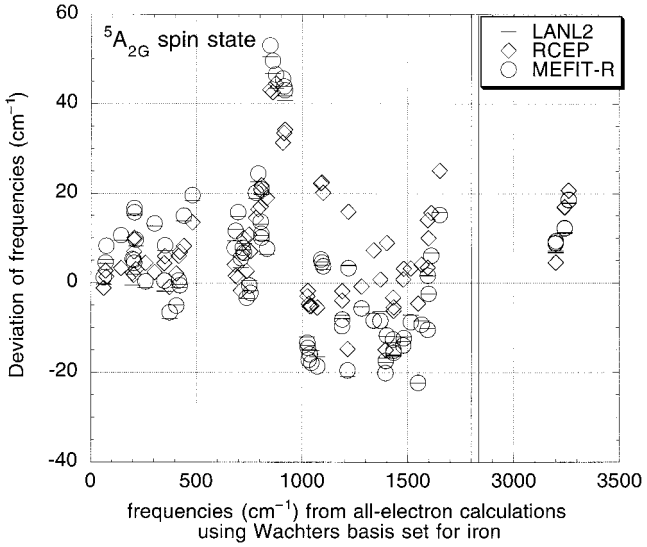

Figure 12. Comparison of frequencies of $^5A_{2G}$ spin state. The frequencies from all-electron calculations using Wachters basis functions are plotted as the ordinate. The *difference* from these values is taken as the abscissa. Circles, diamonds, and bars represent results using the MEFIT-R, RCEP, and LANL2 ECPs. Basis functions used in these calculations are specified in Table 1.

LANL2. We compare first the calculations using Wachters basis functions (column 10 of Table 2) with those using the LANL2 ECPs (column 2 of Table 2). These calculations were carried out at the same geometries (optimized using Wachters basis functions) and with the same basis functions for C, N, and H. They differ in the basis functions for iron and the treatment of core electrons. Except for the $^1A_{1G}$ state, the discrepancies in the relative spin state energies in general fall within the range expected when different basis functions for iron are used (i.e., about 0.1 eV). The agreement between the two types of calculations suggests that core electron correlation and core−valence electron correlation do not vary significantly with respect to the spin states, and are largely canceled out in the relative spin energies. It is likely that the discrepancy for the $^1A_{1G}$ state has a different origin than correlation of core electrons or correlation between core and valence electrons.

The effects of molecular geometries and the basis functions used for C, N, and H may be gauged from comparison between results listed in columns 2 and 5 of Table 2. The latter are calculated from spin state energies at equilibrium geometries, whereas the former are derived from single-point calculations at geometries optimized in all-electron calculations using Wachters basis functions. The basis functions used for C, N, and H are the 6-31G(d) basis functions for the former and the Dunning/Huzinaga valence double-ζ basis[18] for the latter. The results from the two sets of calculations agree to within 0.1 eV, less than that due to differences in the basis functions for iron and in the treatment of core electrons (i.e., with or without ECPs). Similar conclusions may be made based on comparisons of calculations using the RCEPs (columns 3 and 6) and the MEFIT-R ECPs (columns 4 and 7).

For iron, the atomic valence energies calculated using nonrelativistic and relativistic Hartree−Fock calculations differ by about 0.5 eV or less, depending on the electron configuration. We therefore expect that the relative spin state energies calculated using the three types of ECPs agree to

within 0.5 eV. Comparison between columns 2, 3, and 4 of Table 2 shows the effects due to the type of ECPs used in the calculations since the geometry and the basis functions used for C, N, and H in these calculations are the same. These data show very good agreement in general. Notable differences are seen for the $^1A_{1G}$, $^5B_{1G}$, and $^5A_{2G}$ states, but they are nonetheless well below 0.5 eV, the magnitude expected for the relativistic effects. Relativisitc effects are included in the RCEP and MEFIT-R ECPs. The relative energies of the $^1A_{1G}$, $^5B_{1G}$, and $^5A_{2G}$ states based on the RCEP and MEFIT-R ECPs deviate in the same direction from those based on LANL2 ECPs. This suggests that their differences may due in part to the treatment of relativistic effects.

Equilibrium bond lengths (columns 5−7 of Tables 3 and 4) obtained from all-electron calculations with different basis functions for iron agree to within 0.003 Å. Geometries calculated using ECPs are in good agreement with the all-electron calculations. The F−N distances, for example, agree to within 0.01 Å, as found in a previous test of transferability of ab initio ECPs.[5] Large discrepancies between the ECP and the all-electron calculations appear in the distances between the following pairs of atoms: N and C_1, C_1 and C_2, and Fe and C_3. In particular, the values from the ECP calculations are consistently greater than the corresponding all-electron results. This is likely due to the basis functions used for C, N, and H in the ECP calculations. The basis functions for C, N, and H used in the RCEP calculations, for example, do not have the polarization functions used in the all-electron calculations.

Differences in the basis functions for C, N, and H may also explain the contrast between Figures 9 and 10, as well as between Figures 11 and 12—comparison of frequencies from the three ECPs and the two all-electron calculations (SVP and TZV basis functions) with those of all-electron calculations using the Wachters basis set. In particular, significant deviations (>40 cm^{-1}) are observed in the frequency range from 860 to 1000 cm^{-1} for the ECP−Wachters comparisons (Figures 10 and 12) but not for the SVP−Wachters or the TZV−Wachters comparisons (Figures 9 and 11). These vibrational modes involve mainly the out-of-plane bending motion of C_2−H and $C_{2'}$−H in the opposite directions and/or the out-of-plane bending motion of C_3−H.

Experiments on six-coordinated iron porphyrin show that the porphyrin core (Fe−N distance) expands as the spin multiplicity increases.[20−22] Such correlation between structure and spin multiplicity may be the mechanism of spin state modulation in enzyme catalysis.[8] We observed a similar trend in porphyrin core size for the iron(II) porphyrin calculated in all-electron calculations. The ECP calculations successfully reproduce the variation of the "core size" of iron porphyrin (i.e., the Fe−N and the Fe−C_3 distances) with respect to the spin states. This is shown in Figures 13 and 14.

Finally, we compare the timing per SCF iteration for the $^1A_{1G}$ state using the basis functions summarized in Table 1. The CPU time relative to that of all-electron calculations using Wachters basis functions for iron (as ratios) is 0.69, 0.34, 0.99, 0.94, and 1.01 for LANL2, RCEP, MEFIT-R, SVP, and TZV, respectively. Note that the timing comparison presented here does not reflect directly the performance of the ECPs because the basis functions employed for each type of ECP are different.

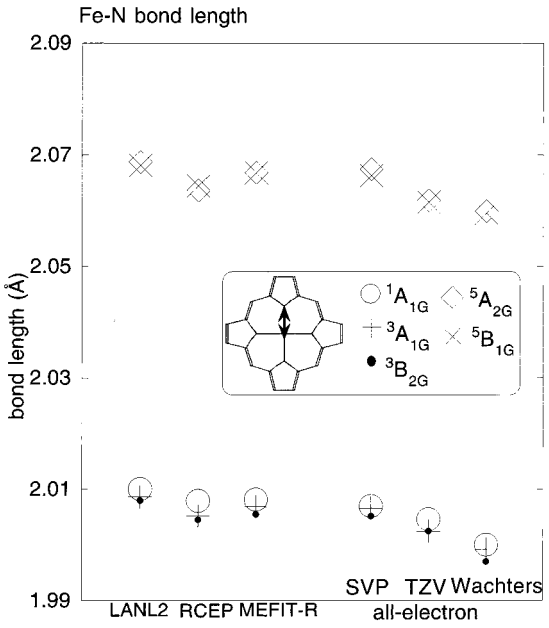

Figure 13. Comparison of porphyrin core size: Fe−N distance. This figure shows the variation of Fe−N distances with respect to the spin states.

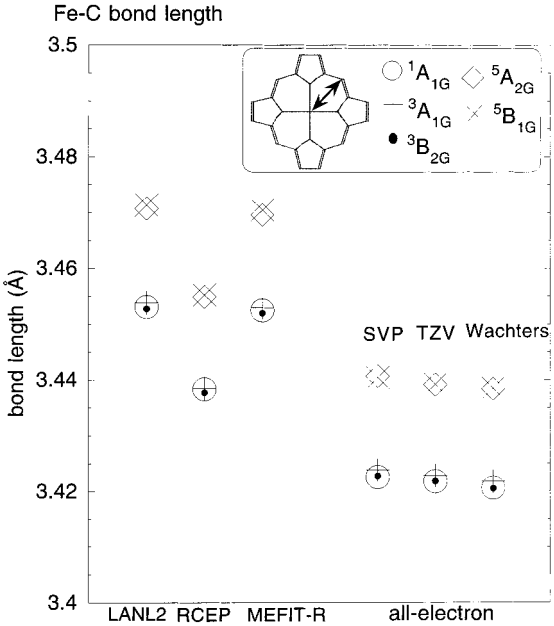

Figure 14. Comparison of porphyrin core size: Fe−C_3 distance. This figure shows the variation of Fe−C_3 distances with respect to the spin states.

V. CONCLUSIONS

Calculations carried out with effective core potentials agree well with all-electron calculations with regard to the energetic ordering of spin states, the variation of the porphyrin size with respect to the spin states, and the vibrational frequencies. Our results suggest that core electron correlation and core−valence electron correlation do not have significant effects on the relative energetics of the spin states of iron porphyrin, or on other molecular properties such as geometries. Our results also suggest that effects of replacing the core electrons with ECPs are much less significant than the choice of basis functions. We conclude that ab initio ECPs such as LANL2, RCEP, and MEFIT-R may be combined with the B3LYP

density functional theory to provide consistent and accurate results.

ACKNOWLEDGMENT

Y.-P.L. is a Cottrell Scholar of the Research Corporation. This work is supported in part by the Research Development Award and the Faculty Research and Creative Activity Support Fund from the Western Michigan University, and a generous donation from the General Motors Company.

REFERENCES AND NOTES

(1) Siegbahn, E. M. Electronic Structure Calculations for Molecules Containing Transition Metals. *Adv. Chem. Phys.* **1996**, *93*, 333−387.
(2) Ziegler, T. Approximate Density Functional Theory as a Practical Tool in Molecular Energetics and Dynamics. *Chem. Rev.* **1991**, *91*, 651.
(3) Blomberg, M. R. A.; Siegbahn, P. E. M.; Svensson, M. Comparison of results from parametrized configuration interaction (PCI-80) and from hybrid density functional theory with experiments for first row transition metal compounds. *J. Chem. Phys.* **1996**, *104*, 9546−9554.
(4) Blomberg, M. R. A.; Siegbahn, P. E. M. A comparative study of high-spin manganese and iron complexes. *Theor. Chem. Acc.* **1997**, *97*, 72−80.
(5) Russo, T. V.; Martin, R. L.; Hay, P. J. Effective Core Potentials for DFT Calculations. *J. Phys. Chem.* **1995**, *99*, 17085−17087.
(6) Glukhovtsev, M.; Bach, R.; Nagel, C. Performance of the B3LYP/ECP DFT calculations of iron-containing compounds. *J. Phys. Chem. A* **1997**, *101*, 316−323.
(7) Dolg, M.; Wedig, U.; Stoll, H.; Preuss, H. Energy-adjusted ab initio pseudopotentials for the first row transition elements. *J. Chem. Phys.* **1987**, *86*, 866−872.
(8) Loew, G.; Dupuis, M. Characterization of a Resting State Model of Peroxidases by an Initio Methods: Optimized Geometries, Electronic Structures, and Relative Energies of the Sextet, Quartet, and Doublet Spin States. *J. Am. Chem. Soc.* **1997**, *119*, 9848−9851.
(9) *Cytochrome P-450, Structure, Mechanism, and Biochemistry*; Oritz de Montellano, P. R., Ed.; Plenum Press: New York, 1986.
(10) Wadt, W. R.; Hay, P. J. Ab initio effective core potentials for molecular calculations. Potentials for K to Au including the outermost core orbitals. *J. Chem. Phys.* **1985**, *82*, 299−310.
(11) Stevens, W. J.; Krauss, M.; Basch, H.; Jasien, P. G. Relativistic compact effective potentials and efficient shared-exponent basis sets for the third-, fourth-, and fifth-row atom. *Can. J. Chem.* **1992**, *70*, 612−630.
(12) Note that the energy-optimized basis functions for LANL2 implemented in Gaussian 98 are slightly different from the ones published in ref 10.
(13) Rappe, A. K.; Smedley, T. A.; Goddard, W. A., III. Flexible d basis sets for Sc through Cu. *J. Phys. Chem.* **1981**, *85*, 2607−2611.
(14) Schäfer, A.; Horn, H.; Ahlrichs, R. Fully optimized contracted Gaussian basis sets for atoms Li to Kr. *J. Chem. Phys.* **1992**, *97*, 2571−2577.
(15) Schäfer, A.; Huber, C.; Ahlrichs, R. Fully optimized contracted Gaussian basis sets of triple-ζ valence quality for atoms Li to Kr. *J. Chem. Phys.* **1994**, *100*, 5829−5835.
(16) Wachters, A. J. H. Gaussian basis set for molecular wave functions containing third-row atoms. *J. Chem. Phys.* **1970**, *52*, 1033−1036.
(17) Hay, P. J. Gaussian basis sets for molecular calculations. The representation of 3d orbitals in transition-metal atoms. *J. Chem. Phys.* **1977**, *66*, 4377−4384.
(18) Dunning, T. H., Jr.; Hay, P. J. In *Modern Theoretical Chemistry*; Schaefer, H. F., III, Ed.; Plenum: New York, 1976; pp 1−28.
(19) Frisch, M. J.; Trucks, G. W.; Schlegel, H. B.; Scuseria, G. E.; Robb, M. A.; Cheeseman, J. R.; Zakrzewski, V. G.; Montgomery, J. A.; Stratmann, R. E.; Burant, J. C.; Dapprich, S.; Millam, J. M.; Daniels, A. D.; Kudin, K. N.; Strain, M. C.; Pomelli, C.; Adamo, C.; Clifford, S.; Ochterski, J.; Petersson, G. A.; Ayala, P. Y.; Cui, Q.; Morokuma, K.; Malick, D. K.; Rabuck, A. D.; Liu, K. G.; Liashenko, A.; Piskorz, P.; Komaromi, I.; Gompers, R.; Martin, R. L.; Fox, D. J.; Keith, T.; Al-Laham, M. A.; Peng, C. Y.; Nanayakkara, A.; Gonzalez, C.; Challacombe, M.; Gill, P. M. W.; Johnson, B. G.; Chen, W.; Wong, M. W.; Andres, J. L.; Head-Gordon, M.; Replogle, E. S.; Pople, J. A. *Gaussian 98*; Gaussian Inc.: Pittsburgh, 1998.
(20) Collman, J. P.; Hoard, J. L.; Kim, N.; Lang, G.; Reed, C. A. *J. Am. Chem. Soc.* **1975**, *97*, 2676.
(21) Radonovich, L.; Bloom, A.; Hoard, J. *J. Am. Chem. Soc.* **1972**, *94*, 2073.
(22) Reed, C. A.; Mashiko, T.; Scheidt, W. R.; Spartalian, K., Lang, G. *J. Am. Chem. Soc.* **1980**, *102*, 2073.

CI000051F